Contribution from the Chemistry Department,
University of Florida, Gainesville, Florida 32611

Use of a Spin-Label Adduct of $Rh_2(pfb)_4$ To Probe the Inductive Effect of Base Coordination through the Metal-Metal Bond[1]

CARL BILGRIEN, RUSSELL S. DRAGO,* JAMES R. STAHLBUSH, and THOMAS C. KUECHLER

Received October 26, 1984

The EPR spectra of the $Rh_2(pfb)_4$·TEMPO adduct (pfb is the perfluorobutyrate anion; TEMPO is the spin-label 2,2,6,6-tetramethylpiperidine-*N*-oxyl) were monitored during complexation with a range of donors to form the species $B{\cdot}Rh_2(pfb)_4{\cdot}$TEMPO in solution. The spin-label probes the influence of donor effects across a metal-metal bond. The data are consistent with a model reported earlier for quantitatively predicting the acidity of the second metal center after a donor has been coordinated to form a 1:1 adduct. For donors capable of only σ type interactions, the observed shift in the spin-label g value was found to be roughly correlated to the enhalpy of adduct formation predicted from the E and C equation. Donors capable of π interactions deviate from the model, in further support of our earlier reports on the back-bonding capabilities of the rhodium carboxylate dimers. The E and C fits of the g values and enthalpies demonstrate that g and ΔH respond in different ways to the E and C properties of the donor. As expected when this is the case, a mediocre linear plot of $-\Delta H$ vs. g results.

Introduction

Previous research from this laboratory on the fundamental aspects of Lewis acid-base interactions has recently been extended to the characterization of Lewis acids containing metal-metal bonds.[2] Measured enthalpies have been incorporated into the E and C correlation,[3] and a quantitative model has been developed for predicting the influence of coordination of the first base on the enthalpy of binding of the second. Metal-metal bonds are characterized in terms of their ability to transmit inductively both covalent and electrostatic effects. The data base used to test this model was small, and a spectroscopic probe was desired to provide a more extensive test.

An earlier EPR study[4] of the nitroxide radical 2,2,6,6-tetramethylpiperidine-*N*-oxyl, TEMPO, provided a correlation between changes in g or A_N and the enthalpy of formation of adducts of this radical with a series of hydrogen-bonding acids. The stronger the ability for hydrogen bonding[4,5] or the more polar[6] a non-hydrogen-bonding solvent the larger the A_N value and the smaller the g value. Adduct foramtion places more paired electron density on the oxygen and more unpaired electron density on the nitrogen of the spin label. We became interested in similar effects upon binding of a spin label to transition-metal clusters of varying Lewis acidity.

In earlier work,[7] the EPR spectrum of the Lewis acid-base adduct of $Rh_2(tfa)_4$ (tfa = trifluoroacetate anion) and TEMPO showed substantial changes in the g and A_N values compared to those of the free radical. These differences and the observation of rhodium hyperfine splitting were attributed to both σ and π interactions of the radical with $Rh_2(tfa)_4$. This interpretation afforded a quantitative estimate of the rhodium d_{xz} contribution to the essentially π orbital of the nitroxide. We have relied on the qualitative MO scheme for 1:1 adducts offered in this earlier paper for interpretation of all our subsequent results.

In the present study, species of the type $B{\cdot}Rh_2(pfb)_4{\cdot}$TEMPO, where B is a coordinated Lewis base, pfb is the perfluorobutyrate anion, and TEMPO is the spin-label, are probed by EPR in order to measure the influence of B on the EPR spectrum of the coordinated nitroxyl radical. The experiment provides an opportunity to study the communication between two dissimilar bases across the Rh-Rh bond. Our model for the transmission of the base-binding effects to the coordinated TEMPO is tested by a successful correlation of the g values with E and C donor parameters.

This investigation also provides support for our synergism model, which claims enhanced π back-bonding from the metal-metal interaction. Several donors containing vacant π-acceptor orbitals have enthalpies of adduct formation with $Rh_2(O_2CR)_4$ dimers[2] in excess of the value predicted for the σ-only interaction by the E and C equation.[3] These findings, along with spectroscopic and electrochemical studies, were used to rationalize additional stabilization in the adduct from metal π^* to ligand π^* back-bonding. Though π back-bonding has often been proposed for the $B-Rh_2$ unit, these studies provided the first quantitative measure of the bond strength enhancement resulting from this type of interaction. The EPR studies described here lend further support to these conclusions.

Relationships between spectral and bonding properties of 1:1 adducts have been reported, such as the linear correlation between $\Delta\nu_{OH}$ and ΔH for a series of 1:1 phenol-base adducts.[8] Breakdown of this correlation upon extension to a larger donor set is attributed to the fundamental differences in $\Delta\nu_{OH}$ and ΔH for gauging E and C effects.[9] Similarly, we show here that the g values for the 2:1 adducts $B{\cdot}Rh_2(pfb)_4{\cdot}$TEMPO are fit by an E and C analysis in that good agreement is observed for experimental and calculated g values from the fit. When g for $B{\cdot}Rh_2(pfb)_4{\cdot}$TEMPO is plotted vs. $\Delta H_{2:1}$ for adduct formation of $B{\cdot}Rh_2(pfb)_4$ with TEMPO, however, a poor correlation results because the two parameters deliver dissimilar C/E ratios. The E and C analysis provides a more appropriate means to correlate the spectroscopic g values.

Experimental Section

Rhodium(II) Perfluorobutyrate ($Rh_2(pfb)_4$). Rhodium(II) acetate ($Rh_2(OAc)_4$) was prepared from $RhCl_3{\cdot}3H_2O$ (Englehard) by literature methods.[10] $Rh_2(pfb)_4$ was prepared from the acetate by exchange with perfluorobutyric acid as follows: Perfluorobutyric acid was distilled at 1 atm since analysis of commercial product showed a substantial hydrogen content. A solution of 2 g of $Rh_2(OAc)_4$ in 30 mL of perfluorobutyric acid and 3.5 mL of perfluorobutyric anhydride was refluxed for a few minutes. Half of the solvent was then distilled off. The remaining solution was cooled to room temperature and then to -20 °C for several hours. The dark blue-green solid $Rh_2(pfb)_4$ was filtered off, washed with pentane, and dried. The product was recrystallized from purified benzene to give 91% yield and stored in a base-free desiccator over P_2O_5 in vacuo. Anal. Calcd for $Rh_2C_{16}O_8F_{28}$: C, 18.17; H, 0.00; F, 50.28. Found: C, 18.63; H, 0.32; F, 49.5. The blue-green solid

(1) Abstracted in part from: Kuechler, T. C. Ph.D. Thesis, University of Illinois, 1977.
(2) (a) Drago, R. S.; Long, J. R.; Cosmano, R. *Inorg. Chem.* **1981**, *20*, 2920. (b) Drago, R. S.; Long, J. R.; Cosmano, R. *Inorg. Chem.* **1982**, *21*, 2196. (c) Drago, R. S. *Inorg. Chem.* **1982**, *21*, 1697.
(3) The empirical E and C equation, $-\Delta H = E_A E_B + C_A C_B$, correlates the enthalpies of adduct formation for a wide range of Lewis acids and bases. Comparison of the E and C predicted enthalpy for σ-bond interaction with the experimentally determined enthalpy can indicate additional contributions to the adduct bond such as steric effects or π back-bonding. For more extensive reviews, see: (a) Drago, R. S. *Coord. Chem. Rev.* **1980**, *33*, 251. (b) Drago, R. S. *Struct. Bonding (Berlin)* **1973**, *15*, 73.
(4) Lim, Y. Y.; Drago, R. S. *J. Am. Chem. Soc.* **1971**, *93*, 891.
(5) Hoffman, B. M.; Eames, T. B. *J. Am. Chem. Soc.* **1969**, *91*, 2169.
(6) Kawamura, T.; Matsunami, S.; Yonezawa, T. *Bull. Chem. Soc. Jpn.* **1967**, *40*, 1111.
(7) Richman, R. M.; Kuechler, T. C.; Tanner, S. P.; Drago, R. S. *J. Am. Chem. Soc.* **1977**, *99*, 1055.
(8) (a) Epley, T. D.; Drago, R. S. *J. Am. Chem. Soc.* **1967**, *89*, 5770. (b) Drago, R. S.; O'Bryan, N.; Vogel, G. C. *Ibid.* **1970**, *92*, 3924. (c) Purcell, K. F.; Drago, R. S. *Ibid.* **1967**, *89*, 2874.
(9) Doan, P. E.; Drago, R. S. *J. Am. Chem. Soc.* **1982**, *104*, 4524.
(10) Legzdins, P.; Mitchell, R. W.; Rempel, G. L.; Ruddick, J. D.; Wilkinson, G. *J. Chem. Soc. A* **1970**, 3322.

0020-1669/85/1324-4268$01.50/0

Table I. EPR Parameters for $Rh_2(pfb)_4$·TEMPO Adducts

complex	g value	10^3A_N,[a] cm^{-1}
Benzene		
TEMPO	2.0052	1.45
$Rh_2(pfb)_4$·TEMPO	2.0163	1.57
$Rh_2(pfb)_4$·TEMPO (ppt)[b]	(2.016)	(1.55)
CH_2Cl_2		
TEMPO	2.0047	1.47
$Rh_2(pfb)_4$·TEMPO	2.0152	1.57
$Rh_2(pfb)_4$·TEMPO (dec)[c]	2.0130	1.54

[a] A_N (cm^{-1}) = $g\beta A_N$ (G) where $\beta = 4.6686 \times 10^{-5}$ cm^{-1} G^{-1} and A_N (G) is the spectral line separation in G. [b] Weak third resonance assigned to observed precipitated complex; parentheses indicate greater range of error. [c] As sealed solution samples aged, a third nitroxide resonance appeared. The nature of this complex is unkown.

contains a small amount of associated water, which can be removed by prolonged drying at 100 °C in vacuum. Anhydrous $Rh_2(pfb)_4$ is a bright yellow-green solid. The blue-green solid is a suitable starting material for the EPR studies herein.

Bases. All bases used were reagent grade and purified to ensure the exclusion of water, usually by distillation from desiccant. TEMPO (2,2,6,6-tetramethylpiperidine-*N*-oxyl, Aldrich) was purified by vacuum sublimation at 25 °C. All sample preparations were performed in a drybox or nitrogen glovebag using P_2O_5 as desiccant.

Solvents. Methylene chloride and benzene were purified by standard methods[11] to ensure the exclusion of water. Solvents were degassed by freeze–pump–thaw cycles prior to use.

EPR Spectroscopy. Spectra were recorded with Varian E-9 (X-band) and E-15 (Q-band) spectrometers. A Hewlett-Packard gaussmeter was used to determine the field homogeneity and the exact positions of the resonances in the Q-band spectra. 2,2-Diphenyl-1-picrylhydrazyl (DPPH) was used as an external reference for the X-band spectra. Solutions were prepared ca. 5.0×10^{-3} M in $Rh_2(pfb)_4$, 4.5×10^{-3} M in base, and 5.0×10^{-4} M in TEMPO in methylene chloride or benzene. Spectra were recorded at 25 or 80 °C. At ambient temperture, complex precipitation was often a problem at these concentrations in benzene solution.

Results and Discussion

Characterization and EPR Spectra of $Rh_2(pfb)_4$·TEMPO. TEMPO is a donor of moderate strength that does not bind to $Rh_2(OAc)_4$ or $Rh_2(but)_4$ (but = butyrate) but forms adducts with the corresponding fluorinated derivatives, $Rh_2(tfa)_4$ and $Rh_2(pfb)_4$. A calorimetric titration of $Rh_2(pfb)_4$ with TEMPO in benzene showed that even at 5:1 TEMPO:acid mole ratio, the data fit a 1:1 equilibrium well to yield $-\Delta H_1 = 12.5$ kcal mol^{-1} (uncorrected for benzene solvation) and $K_1 = 81$ L mol^{-1}. Thus the equilibrium constant for the addition of a second nitroxide base is quite small, and the EPR spectra were assigned accordingly.

The Q-band EPR parameters for TEMPO in benzene and CH_2Cl_2 are listed in Table I. The X-band EPR spectrum for TEMPO in CH_2Cl_2 is shown in Figure 1a. The expected three-line pattern for one unpaired electron interacting with one nitrogen nucleus (^{14}N, $I = 1$) is centered at $g = 2.0047$ by using DPPH ($g = 2.002\,32$) as the reference.

The Q-band EPR spectrum of $Rh_2(pfb)_4$·TEMPO in CH_2Cl_2 is shown in Figure 1b. The triplet at high field is assigned to the solvated TEMPO. Two additional resonances are located downfield. The first, more intense triplet centered at $g = 2.0152$ is attributed to the nitroxide resonance of $Rh_2(pfb)_4$·TEMPO. The second, less intense triplet is due to an uncharacterized decomposition product. Sealed samples under dinitrogen exhibited growth of this signal with concomitant loss of the $Rh_2(pfb)_4$·TEMPO signal. After 4 days, the two signals were of equal intensity.

The Q-band EPR spectrum of $Rh_2(pfb)_4$·TEMPO in benzene is shown in Figure 1c. Significant differences between the spectra obtained in CH_2Cl_2 and those in benzene are evident. Most notable is the ratio of intensities for the bound and the free TEMPO resonances. In both solvents, the molar ratio of $Rh_2(pfb)_4$ to TEMPO was 10:1. Methylene chloride, however, competes as a Lewis acid with $Rh_2(pfb)_4$ for TEMPO while benzene[12] competes as a donor with TEMPO for $Rh_2(pfb)_4$. The equilibrium constant for adduct formation in CH_2Cl_2 approximated from the areas beneath the resonances in Figure 1b is 7×10^2 mol^{-1}, roughly 1 order of magnitude larger than in benzene. A third triplet is observed in the benzene solution spectrum, overlapping the solution resonance of $Rh_2(pfb)_4$·TEMPO. This weak signal is assigned to a small amount of precipitated adduct, for it has a similar g value and hyperfine splitting but is a broader resonance.

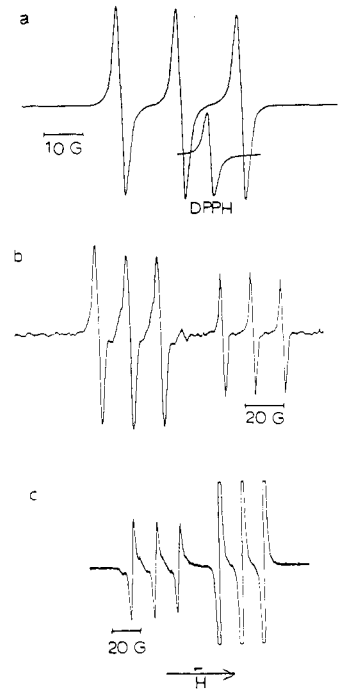

Figure 1. EPR spectra of TEMPO and some $Rh_2(pfb)_4$ adducts: (a) X-band EPR of TEMPO in CH_2Cl_2; (b) Q-band EPR of $Rh_2(pfb)_4$ with TEMPO in CH_2Cl_2; (c) Q-band EPR of $Rh_2(pfb)_4$ with TEMPO in benzene.

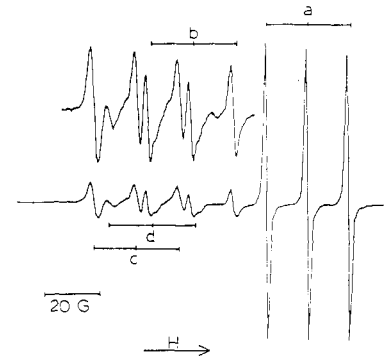

Figure 2. Sample Q-band EPR spectrum observed for a CH_2Cl_2 solution of $Rh_2(pfb)_4$, TEMPO, and DMA. Species observed: (a) free TEMPO; (b) DMA·$Rh_2(pfb)_4$·TEMPO; (c) $Rh_2(pfb)_4$·TEMPO; (d) precipitated $Rh_2(pfb)_4$·TEMPO.

Rhodium hyperfine splitting was observed in the benzene solution spectra ($A_{Rh} = 1.5$ G) but not in the CH_2Cl_2 solution spectra. The observed rhodium hyperfine splitting in a rhodium dimer/TEMPO adduct has been rationalized[7] in terms of mixing of a Rh d_{xz} orbital with the π^* nitroxide orbital containing the unpaired electron spin. The absence of observable Rh hyperfine splitting in the CH_2Cl_2 solutions is due to the broader resonance line width in this solvent. Attempts to raise the temperature to narrow the line width of the CH_2Cl_2 spectra were limited by the low boiling point of CH_2Cl_2 (40 °C).

(11) Gordon, A. J.; Ford, R. A. "The Chemist's Companion"; Wiley: New York, 1972.

(12) Drago, R. S.; Parr, L. B.; Chamberlain, C. S. *J. Am. Chem. Soc.* **1977**, *99*, 3202.

Table II. EPR Parameters of B·$Rh_2(pfb)_4$·TEMPO in Benzene Solution

B	10^3A_N, cm^{-1}	g
no base	1.570	2.0163
ethyl acetate	1.570	2.0133
acetone	1.545	2.0127
bridged ether[a]	1.565	2.0123
tetrahydrofuran	1.560	2.0123
hexamethylphosphoramide	1.545	2.0119
dimethyl sulfoxide	1.580	2.0118
dimethylformamide	1.550	2.0115
acetonitrile	1.570	2.0112
pyridine	1.575	2.0086
N-methylimidazole	1.570	2.0084
4-picoline	1.540	2.0082
dimethylthioformamide	*c*	2.0079
piperidine	*c*	2.0079
dimethylacetamide[b]		2.0119
triphenylphosphine oxide	1.575	2.0124
diphenylformamide	1.560	2.0122
triphenylarsine oxide	1.550	2.0110
diphenylamine	1.568	2.0105
triphenylphosphine sulfide	1.540	2.0097
carbon monoxide	1.540	2.0092

[a] 7-Oxabicyclo[2.2.1]heptane. [b] Reference 15. [c] Unresolved.

EPR Spectra of B·$Rh_2(pfb)_4$·TEMPO. Typically, solutions were prepared in a 9:10:1 molar ratio of base:rhodium complex:TEMPO in O_2-free benzene and CH_2Cl_2. Most of the nitroxide existed in the unbound state, while the coordinated nitroxide existed as the B·$Rh_2(pfb)_4$·TEMPO species. With some of the bases, it was possible to observe simultaneously the EPR spectrum of all three nitroxide species (free TEMPO, $Rh_2(pfb)_4$·TEMPO and B·$Rh_2(pfb)_4$·TEMPO). A representative spectrum for dimethylacetamide in CH_2Cl_2 solution with $Rh_2(pfb)_4$ and TEMPO is shown in Figure 2. In all cases, the signal for the B·$Rh_2(pfb)_4$·TEMPO species appeared between those for the free nitroxide and $Rh_2(pfb)_4$·TEMPO. The nitrogen hyperfine splitting for these 2:1 adducts was usually either equal to or slightly less than that observed for the $Rh_2(pfb)_4$·TEMPO adduct. Both the above effects are expected from an inductive weakening of the rhodium–nitroxide bond by the coordinated base.[2] No rhodium hyperfine splitting was resolved for any of the B·$Rh_2(pfb)_4$·TEMPO adducts. A wide range of g values was observed for mixed-donor 2:1 adducts. Furthermore, the g value is sensitive to minor changes in B, and it is possible to distinguish diphenylformamide from dimethylformamide, triphenylphosphine oxide from triphenylarsine oxide, and pyridine from 4-picoline. A tabulation of the EPR parameters in benzene is given in Table II. Earlier studies[2] from this laboratory have shown the existence of complicating contributions to measured enthalpies in benzene for the rhodium butyrate system from solvent coordination and acid aggregation. Accordingly, the EPR measurements for bases in the E and C correlation were repeated in CH_2Cl_2 and are summarized in Table III. The g and A_N values are similar in both solvents, but only the g values change appreciably with donor. A qualitative discussion of the trends follows.

The contributions to the shift in the g value as a function of base binding can be understood in terms of the MO description[7] for the $Rh_2(pfb)_4$·TEMPO adduct shown in Figure 3. Bonding in $Rh_2(pfb)_4$·TEMPO has been described in terms of σ donation from a nitroxide oxygen lone pair into the Rh d_{z^2} (σ^*) orbital with concomitant orbital mixing of the Rh d_{xz} (π^*) orbital with the nitroxide π^* orbital containing the unpaired spin. When B is a σ donor, the metal–nitroxide bond is weakened, and the g value moves toward that of free nitroxide. When B is a π acceptor the metal–nitroxide bond can be weakened in two ways. Directly, competition for M–M π^* electron density decreases the π back-bonding to TEMPO. Indirectly, a π acceptor exhibits enhanced σ donation, causing weakening of the metal–nitroxide bond in the same way as a pure σ donor. The net result is that σ donors and π acceptors both serve to weaken the metal nitroxide bond and cause a lowering of the g value back toward the free solution value of TEMPO. Note the appreciably lowered g value observed when B is the poorly σ-donating and good π-accepting CO ligand.

Table III. Correlation of EPR Parameters of B·$Rh_2(pfb)_4$·TEMPO in CH_2Cl_2 Solution with $\Delta H^{1:1}$ and $\Delta H^{2:1}$

B	10^3A_N, cm^{-1}	g[a]	g_{calcd}[b]	$-\Delta H_B^{1:1}$,[c] kcal mol^{-1}	$-\Delta H_T^{2:1}$,[d] kcal mol^{-1}
no base	1.57	2.0152	2.0152	0	15.4
methyl acetate	1.55	2.0128	2.0130	7.37	14.1
ethyl acetate	1.55	2.0127	2.0129	7.96	14.0
acetone	1.55	2.0122	2.0125	9.05	13.9
p-dioxane	1.55	2.0120	2.0122	9.66	13.7
dimethylacetamide	1.55	2.0119	2.0119	11.17	13.5
bridged ether[e]	1.55	2.0119	2.0114	11.64	13.6
tetrahydrofuran	1.55	2.0118	2.0111	12.38	13.4
dimethyl sulfoxide	1.55	2.0116	2.0117	11.74	13.4
hexamethylphosphoramide	1.55	2.0115	2.0109	13.87	13.0
dimethylformamide	1.55	2.0114	2.0120	10.54	13.6
acetonitrile	1.56	2.0108	(2.0132)[g]	6.81	14.2
pyridine *N*-oxide	1.55	2.0101	2.0106	14.65	13.0
cage phosphite[f]	1.56	2.0095	(2.0104)[g]	13.93	13.4
diethyl sulfide	1.55	2.0093	(2.0100)[g]	14.59	13.4
4-picoline	1.55	2.0083	(2.0092)[g]	17.75	12.6
pyridine	1.56	2.0081	(2.0096)[g]	17.06	12.8
1-methylimidazole	1.56	2.0079	2.0081	20.32	12.4
piperidine	*h*	2.0074	2.0078	21.28	12.3
triethylamine	*h*	2.0069	2.0068	24.31	11.9

[a] g(B·$Rh_2(pfb)_4$·TEMPO). [b] g calculated from eq 4 by using $C_A^{1:1}$ and $E_A^{1:1}$ from eq 2 and 3 and values reported in Table IV. [c] Calculated enthalpy for adding B to $Rh_2(pfb)_4$ from values in Table IV. [d] Calculated enthalpy for adding TEMPO to $Rh_2(pfb)_4$·B using $E_A^{1:1}$ and $C_A^{1:1}$ from eq 2 and 3 along with the values in Table IV. [e] 7-Oxabicyclo[2.2.1]heptane. [f] 4-Ethyl-1-phospha-2,6,7-trioxabicyclo-[2.2.2]octane. [g] Systems in which metal π^* to ligand π^* back-bonding occurs.[2] [h] Unresolved.

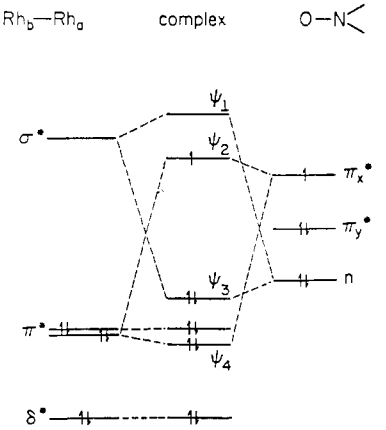

Figure 3. Qualitative MO diagram of the 1:1 adduct of $Rh_2(tfa)_4$ with TEMPO. MO's Ψ_1 through Ψ_4 comprise the major contributions in the analysis.

The absence of ^{103}Rh hyperfine splitting in spectra of the B·$Rh_2(pfb)_4$·TEMPO adducts is understandable. The observed rhodium coupling[7] in $Rh_2(tfa)_4$·TEMPO is barely resolvable and is attributed primarily to spin polarization of the rhodium nitroxide bond. Addition of a second base weakens the rhodium–nitroxide σ bond, leading to an even smaller rhodium hyperfine coupling.

The general trends in the nitrogen hyperfine splitting can be interpreted by the same bonding considerations as those for g. A

Table IV. *E* and *C* Parameters for Species Used in This Study

B	E_B	C_B	$E_A^{1:1}$	$C_A^{1:1}$
methyl acetate	0.903	1.61	4.01	1.68
ethyl acetate	0.975	1.74	3.93	1.68
acetone	0.987	2.33	3.92	1.66
p-dioxane	1.09	2.38	3.80	1.65
dimethylacetamide	1.32	2.58	3.53	1.65
bridged ether	0.887	4.11	4.03	1.59
tetrahydrofuran	0.978	4.27	3.93	1.58
dimethyl sulfoxide	1.34	2.85	3.51	1.64
hexamethylphosphoramide	1.52	3.55	3.30	1.61
dimethylformamide	1.23	2.48	3.63	1.65
acetonitrile	0.886	1.34	4.03	1.69
pyridine *N*-oxide	1.34	4.52	3.51	1.58
cage phosphite	0.548	6.41	4.42	1.51
diethyl sulfide	0.339	7.40	4.67	1.47
4-picoline	1.17	6.80	3.70	1.49
pyridine	1.17	6.40	3.70	1.51
1-methylimidazole	0.934	8.96	3.98	1.41
piperidine	1.01	9.29	3.89	1.40
triethylamine	0.991	11.09	3.91	1.34
TEMPO	0.915	6.21	4.00	1.51

A	E_A	C_A	*k*	*k'*
$Rh_2(pfb)_4$	5.06	1.74	1.16	0.0364

strong σ donor, B, weakens the metal–nitroxide interaction, decreasing A_N compared to the case of no base present. Quantitative correlations were not very satisfactory, indicating that complicating factors contribute to A_N. For most of the nitrogen donor bases, a small additional hyperfine splitting is evident for the $B{\cdot}Rh_2(pfb)_4{\cdot}$TEMPO adduct. Though not well resolved, computer simulations indicate this splitting resembles that from a nitrogen nucleus with $I = 1$. The molecular orbital bonding the rhodium dimer "acceptor" σ^* orbital to the two bases is delocalized over both of the coordinated bases, and spin polarization of this σ MO by unpaired spin on the nitroxide leads to unpaired spin density on the nitrogen atom of the second base.

Quantitative Correlations of the EPR Parameters with the Donor Strength of B. The general trends discussed in the previous section suggest that *g* values from the EPR spectra may be used to provide quantitative data about the strength of binding. This encouraged us to investigate the quantitative relationship between the enthalpy of adduct formations and changes in the A_N and *g* values. The CH_2Cl_2 data will be used in all correlations. Recently a model has been proposed[2] and tested for predicting the enthalpy of coordination of a second donor, B, to an $M_2(O_2CR)_4{\cdot}B$ adduct to form a 2:1 adduct. In this model, the E_A parameter for the 1:1 adduct behaving as an acid to form a 2:1 adduct, $E_A^{1:1}$, is given by

$$E_A^{1:1} = E_A - kE_B \tag{1}$$

and $C_A^{1:1}$ is given by

$$C_A^{1:1} = C_A - k'C_B \tag{2}$$

where *k* and *k'* reflect (for σ donors) the effectiveness of the metal–metal bond at transmitting the inductive influence of base coordination to the second metal center. $E_A^{1:1}$ and $C_A^{1:1}$ values for $B{\cdot}Rh_2(pfb)_4$ can be calculated from eq 1 and 2. The reported *E* and *C* values[2,3] used in this analysis are given in Table IV. Additionally, the *E* and *C* parameters have shown utility in correlating spectral parameters by writing

$$\Delta\chi + W = E_AE_B^* + C_AC_B^* \tag{3}$$

for the case where a base is held constant and a series of acids studied. The asterisks imply that conversion units for converting E_A from $(\text{kcal mol}^{-1})^{1/2}$ are included in E_B^* along with the response to the quantity measured induced in the base by the acid. The *W* term[13,14] incorporates any constant contribution to the measured parameter in all systems studied.

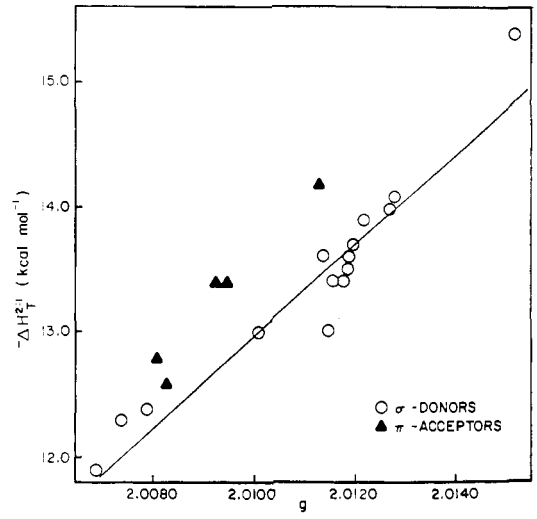

Figure 4. Correlation of predicted enthalpy of adduct formation, $\Delta H_T^{2:1}$, for $Rh_2(pfb)_4{\cdot}B$ and TEMPO to the observed *g* value of $B{\cdot}Rh_2(pfb)_4{\cdot}$TEMPO: (○) σ donors; (▲) π acceptors. Character size represents range of experimental error. The best fit line is for σ donors (eq 6).

With eq 3, we can demonstrate the utility of the inductive transfer model (eq 1 and 2) to describe the transfer of coordination effects through the metal–metal bond. From eq 1 and 2, $E_A^{1:1}$ and $C_A^{1:1}$ of the various $B{\cdot}Rh_2(pfb)_4$ adducts are calculated and listed in Table IV. Note how the acid parameters decreases as the inductive effect increases. With these *E* and *C* values for the various 1:1 adducts, we are now in a position to attempt a correlation of the *g* values obtained when TEMPO is coordinated to the second coordination position to form a series of 2:1 adducts of general formula $B{\cdot}Rh_2(pfb)_4{\cdot}$TEMPO. The equation

$$g + W = E_A^{1:1}E_B^* + C_A^{1:1}C_B^* \tag{4}$$

is used where *g* has been substituted for $\Delta\chi$ in eq 3. The simultaneous equations are solved for E_B^* and C_B^*, which are the spectroscopic parameters for TEMPO needed to predict *g*. The quantity *W* includes the *g* value for free TEMPO (2.0047) as well as any nonzero enthalpy components of the spectroscopic relation.[9,13] The best-fit results yield

$$E_B^* = 1.16 \times 10^{-3}\ (0.29 \times 10^{-3})$$

$$C_B^* = 1.78 \times 10^{-2}\ (0.10 \times 10^{-2}) \qquad W = -1.9784\ (0.0018)$$

with standard deviations in parentheses. Table III contains the *g* values calculated from this fit (g_{calcd}). The columns of *g* and g_{calcd} show excellent agreement, generally within the accuracy of the measured numbers, except in those cases where metal $\pi^* \rightarrow$ B back-bonding occurs (data in parentheses). The close agreement between *g* and g_{calcd} demonstrates that the inductive model (eq 1 and 2) adequately describes the transmission of coordination effects through the metal–metal bond, for it is this model that describes the varying acidity of the second metal center. The deviation of the π-acceptor bases in terms of stabilization at the B·Rh adduct bond lends further support to the π-back-bonding abilities of the Rh_2^{4+} unit.[2]

To see if a relationship exists between *g* and the strength of TEMPO binding to $B{\cdot}Rh_2(pfb)_4$, enthalpies for binding TEMPO were calculated from

$$-\Delta H_T^{2:1} = E_A^{1:1}E_B + C_A^{1:1}C_B \tag{5}$$

The calculated enthalpies are listed in Table III, and the plot of $\Delta H_T^{2:1}$ vs. *g* is illustrated in Figure 4. A least-squares analysis of the 15 data points for σ-only donors yields

$$-\Delta H_T^{2:1} = 365.8g - 722.3 \tag{6}$$

$$n = 15 \qquad r = 0.959$$

(13) Drago, R. S.; Kroeger, M. K.; Stahlbush, J. R. *Inorg. Chem.* **1981**, *20*, 306.
(14) (a) Guidry, R. M.; Drago, R. S. *J. Am. Chem. Soc.* **1973**, *95*, 759. (b) Li, M. P.; Drago, R. S. *J. Am. Chem. Soc.* **1976**, *98*, 5129.
(15) Li, M. P. Ph.D. Thesis, University of Illinois, 1976.

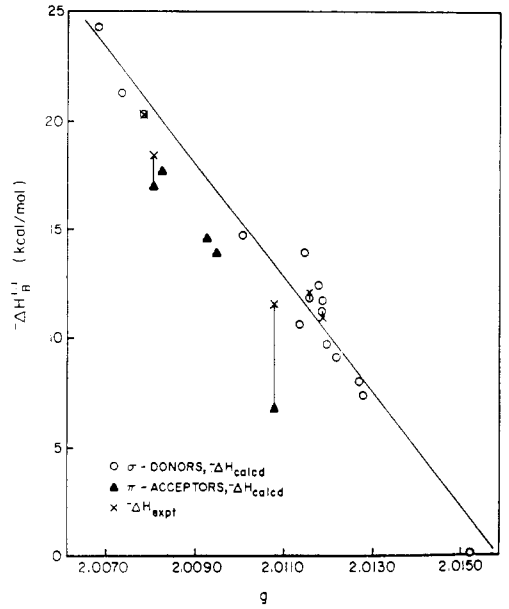

Figure 5. Correlation of predicted enthalpy of adduct formation, $\Delta H_B^{1:1}$, for $Rh_2(pfb)_4$ and donor, B, to the observed g value of $B{\cdot}Rh_2(pfb)_4{\cdot}$TEMPO: (○) σ donors; (▲) π acceptors. For those systems where $\Delta H_B^{1:1}$ has been experimentally determined, the corresponding experimental heats are given by X. Character size indicates range of experimental error. The best-fit line is for σ donors (eq 8).

As discussed earlier, correlation coefficients can be very misleading,[14] and acceptance of this correlation would lead to several misses of 0.3 kcal mol^{-1} or more. We find the very interesting result that the $\Delta H_T^{2:1}$ values fit the E and C equation as do the g values, but a linear plot is not obtained when $\Delta H_T^{2:1}$ is plotted vs. g. In earlier reports[9,13] from this laboratory, we have shown that in order to obtain a straight-line plot of ΔH vs. a spectral shift for a wide range of donors interacting with one acid, the C/E ratio from the enthalpy correlations and that from the spectral shift (eq 3) must be comparable. That is, for the correlation to have physical significance here, both $\Delta H_T^{2:1}$ and g must respond similarly to covalent and electrostatic properties of the coordinated donor. The C_B/E_B ratio for TEMPO used to fit g is 13.8. The C_B/E_B value for TEMPO from experimental enthalpies[3] used to calculate $\Delta H_T^{2:1}$ is 6.8. The difference is great enough to expect a poor linear correlation between g and $\Delta H_T^{2:1}$.

One final point of importance comes from this study, the ability of the g values to gauge the effect of metal $\pi^* \rightarrow$ B back-bonding. The E and C parameters are derived from σ-only interactions, and hence the calculated ΔH values in Table III reflect only the σ component of the adduct bond. The experimental g values, however, reflect the sum of σ-donor and any π-acceptor interactions. In Figure 5, the enthalpies of 1:1 adduct formation for $B{\cdot}Rh_2(pfb)_4$ are plotted as a function of the experimental g values for the 2:1 adducts $B{\cdot}Rh_2(pfb)_4{\cdot}$TEMPO. Both calculated (○, ▲) and experimental (×) enthalpies are included. In Figure 5, the calculated (σ-only) enthalpies are all lower than the g values would suggest for the five donors that act as π acceptors: acetonitrile, cage phosphite, diethyl sulfide, 4-picoline, and pyridine. Additional stabilization in the $B{\cdot}Rh_2(pfb)_4$ adduct bond is consistent with Rh $\pi^* \rightarrow$ B back-bonding. In the two cases where experimental $\Delta H_B^{1:1}$ values are available[2] (acetonitrile and pyridine), the measured heats lie much closer to the correlation line. Thus, the g values manifest both σ and π effects across the metal–metal bond, both serve to lower the g value of coordinated TEMPO, and σ donation appears to exert a stronger influence than π acceptance. (Inclusion of π effects brings $\Delta H_B^{1:1}$ closer to the correlation line but not all the way.)

In a related study,[16] the effect of donors upon coordinated CO in 2:1 adducts of the type $B{\cdot}Rh_2(pfb)_4{\cdot}CO$ has been probed by IR.

Conclusion

A coordinated spin label has been used to monitor donor trans influence across a metal–metal bond. Experimental g values vary regularly with donor strength. When donor effects are taken into account with our inductive transfer model to describe the perturbation of the rhodium dimer acidity, the calculated g values lie in good agreement with the experiment, providing added support for this model. Systematic deviations for π acceptors are consistent with the Rh_2^{4+} interacting in a π-back-bonding fashion. The dependence of enthalpy/spectral parameter correlation linearity upon the C/E ratios of the plotted parameters has been further illustrated.

Acknowledgment. The authors acknowledge the support of this research by the National Science Foundation, Grant No. 84-08149, and thank Dr. Glenn C. Vogel and Dr. Roger Cramer for helpful discussions.

Registry No. TEMPO, 2564-83-2; $B{\cdot}Rh_2(pfb)_4{\cdot}$TEMPO (B = ethyl acetate), 98942-19-9; $B{\cdot}Rh_2(pfb)_4{\cdot}$TEMPO (B = acetone), 98942-20-2; $B{\cdot}Rh_2(pfb)_4{\cdot}$TEMPO (B = 7-oxabicyclo[2.2.1]heptane), 98942-21-3; $B{\cdot}Rh_2(pfb)_4{\cdot}$TEMPO (B = tetrahydrofuran), 98942-22-4; $B{\cdot}Rh_2(pfb)_4{\cdot}$TEMPO (B = hexamethylphosphoramide), 98942-23-5; $B{\cdot}Rh_2(pfb)_4{\cdot}$TEMPO (B = dimethyl sulfoxide), 98942-24-6; $B{\cdot}Rh_2(pfb)_4{\cdot}$TEMPO (B = dimethylformamide), 98942-25-7; $B{\cdot}Rh_2(pfb)_4{\cdot}$TEMPO (B = acetonitrile), 98942-26-8; $B{\cdot}Rh_2(pfb)_4{\cdot}$TEMPO (B = pyridine), 98942-27-9; $B{\cdot}Rh_2(pfb)_4{\cdot}$TEMPO (B = *N*-methylimidazole), 98942-28-0; $B{\cdot}Rh_2(pfb)_4{\cdot}$TEMPO (B = 4-picoline), 98942-29-1; $B{\cdot}Rh_2(pfb)_4{\cdot}$TEMPO (B = dimethylthioformamide), 98942-30-4; $B{\cdot}Rh_2(pfb)_4{\cdot}$TEMPO (B = piperidine), 98942-31-5; $B{\cdot}Rh_2(pfb)_4{\cdot}$TEMPO (B = triphenylphosphine oxide), 98942-32-6; $B{\cdot}Rh_2(pfb)_4{\cdot}$TEMPO (B = diphenylformamide), 98942-33-7; $B{\cdot}Rh_2(pfb)_4{\cdot}$TEMPO (B = triphenylarsine oxide), 98942-34-8; $B{\cdot}Rh_2(pfb)_4{\cdot}$TEMPO (B = diphenylamine), 98942-35-9; $B{\cdot}Rh_2(pfb)_4{\cdot}$TEMPO (B = triphenylphosphine sulfide), 98942-36-0; $B{\cdot}Rh_2(pfb)_4{\cdot}$TEMPO (B = carbon monoxide), 98942-37-1; $B{\cdot}Rh_2(pfb)_4{\cdot}$TEMPO (B = methyl acetate), 98942-38-2; $B{\cdot}Rh_2(pfb)_4{\cdot}$TEMPO (B = *p*-dioxane), 98942-39-3; $B{\cdot}Rh_2(pfb)_4{\cdot}$TEMPO (B = pyridine *N*-oxide), 98942-40-6; $B{\cdot}Rh_2(pfb)_4{\cdot}$TEMPO (B = 4-ethyl-1-phospha-2,6,7-trioxabicyclo[2.2.2]octane), 98942-41-7; $B{\cdot}Rh_2(pfb)_4{\cdot}$TEMPO (B = diethyl sulfide), 98942-42-8; $B{\cdot}Rh_2(pfb)_4{\cdot}$TEMPO (B = triethylamine), 98942-43-9; $B{\cdot}Rh_2(pfb)_4{\cdot}$TEMPO (B = dimethylacetamide), 98942-44-0; $Rh_2(pfb)_4{\cdot}$TEMPO, 98942-18-8; $Rh_2(pfb)_4$, 81028-20-8; Rh, 7440-16-6; $B{\cdot}Rh_2(pfb)_4$ (B = methyl acetate), 99232-13-0; $B{\cdot}Rh_2(pfb)_4$ (B = ethyl acetate), 99232-14-1; $B{\cdot}Rh_2(pfb)_4$ (B = acetone), 99232-15-2; $B{\cdot}Rh_2(pfb)_4$ (B = *p*-dioxane), 99232-16-3; $B{\cdot}Rh_2(pfb)_4$ (B = dimethylacetamide), 93084-74-3; $B{\cdot}Rh_2(pfb)_4$ (B = 7-oxabicyclo[2.2.1]heptane, 99232-17-4; $B{\cdot}Rh_2(pfb)_4$ (B = tetrahydrofuran), 99232-18-5; $B{\cdot}Rh_2(pfb)_4$ (B = dimethyl sulfoxide), 93084-71-0; $B{\cdot}Rh_2(pfb)_4$ (B = hexamethylphosphoramide), 99232-19-6; $B{\cdot}Rh_2(pfb)_4$ (B = dimethylformamide), 99232-20-9; $B{\cdot}Rh_2(pfb)_4$ (B = acetonitrile), 93084-73-2; $B{\cdot}Rh_2(pfb)_4$ (B = 4-ethyl-1-phospha-2,6,7-trioxabicyclo-[2.2.2]octane), 99232-21-0; $B{\cdot}Rh_2(pfb)_4$ (B = diethyl sulfide), 99232-22-1; $B{\cdot}Rh_2(pfb)_4$ (B = pyridine *N*-oxide), 99232-23-2; $B{\cdot}Rh_2(pfb)_4$ (B = 4-picoline), 99248-48-3; $B{\cdot}Rh_2(pfb)_4$ (B = pyridine), 93084-72-1; $B{\cdot}Rh_2(pfb)_4$ (B = 1-methylimidazole), 93110-20-4; $B{\cdot}Rh_2(pfb)_4$ (B = piperidine), 99232-24-3; $B{\cdot}Rh_2(pfb)_4$ (B = triethylamine), 99232-25-4.

(16) Bilgrien, C.; Drago, R. S.; Vogel, G. C.; Stahlbush, J. R., to be submitted for publication.